BECN1 modulates hematopoietic stem cells by targeting Caspase-3-GSDME-mediated pyroptosis

Xiuxiu Yang[a], Liang Ge[b], Jianwei Wang[a,c,*]

[a]School of Pharmaceutical Sciences, Tsinghua University, Beijing 100084, China.; [b]School of Life Sciences, Tsinghua University, Beijing 100084, China.; [c]Beijing Advanced Innovation Center for Structural Biology, Tsinghua University, Beijing 100084, China

Abstract

Hematopoietic stem cells (HSCs) maintain the blood system throughout the lifespan. However, the molecular mechanism maintaining HSC character remains not fully understood. In this study, we observed that the targeted deletion of *Becn1* disrupts the blood system and impairs the reconstitution capacity of HSCs. Interestingly, *Becn1* deletion did not lead to dysfunction of autophagy in HSCs, indicating a non-classical role of BECN1 in regulating HSCs function. While we observed the increase of Caspase-3-GSDME-mediated pyroptosis in *Becn1* deficient hematopoietic stem and progenitor cells. Forced expression of the full-length GSDME compromises the function of HSCs. In brief, we identified a novel role of *Becn1* in modulating HSCs by regulating pyroptosis, but not through autophagy. This study provides a new link between BECN1-Caspase-3-GSDME signaling and HSC maintenance.

Keywords: Autophagy, Becn1, Cell death, Hematopoietic stem cell, Pyroptosis

1. INTRODUCTION

Hematopoietic stem cells (HSCs) are a rare but long-lived population of blood cells.[1] HSCs lie on the top of the blood system and give rise to all lineages of blood cells throughout the lifespan. Since the life-span of most mature blood cells are limited, maintenance of blood homeostasis almost relies on the self-renewal and differentiation ability of HSCs.[1] HSCs locate far from the blood vessel,[2–5] a niche relative shortage of nutrient and oxygen, and are metabolically inactive, which is considered to be indispensable for maintaining of HSCs.[6–8] Disrupting the inactive metabolic state by targeting pyruvate dehydrogenase kinase (Pdk) reduced glycolysis, quiescence and reconstitution ability of HSC.[7] While *Pdk* deletion was reported to inhibit the Acetyl-coenzyme A (AcCoA) depletion, both of which were involved in starvation-induced macroautophagy (hereafter called autophagy).[9] Transcription factor FOXO3A protected HSCs to survive from metabolic stress via autophagy promotion. Autophagy gene *Atg12* helped HSC to stay an inactive metabolic and functional state by metabolically activated mitochondria removing.[8] Thus, under a specific niche environment, autophagy plays an important role in keeping the stemness of HSCs by metabolic modulation.

Autophagy is a highly conserved process of catabolism induced by various cellular stress,[10] and plays an important role in maintaining the function of lots of stem cells, including HSCs.[11] Autophagy is mediated by series of evolution-conserved autophagy-related (ATG) genes, such as *Ulk1*, *FIP200*, *Becn1*, *Atg9a*, *Atg14*, *Atg5*, *Atg7*, and *Atg12*.[11] Previous reports showed that FIP200, which participates in autophagy initiation, was required for fetal HSCs maintenance.[12] ATG5, ATG7, and ATG12, which are involved in autophagy vesicle elongation, are essential in maintaining adult HSCs.[8,13,14] *Becn1*, one of the first identified autophagy genes found in mammalian and an ortholog of *Atg6* in yeast, participates in phagophore nucleation, expansion, and also the non-autophagic process which is endosome maturation.[11,15,16] *Becn1* is unique among the ATGs because of its autophagy-independent function.[17]*Becn1* contains a Bcl-2-homology-3 (BH3)-only domain,[18] a domain that usually plays a role in mediating cell death[18] and recent studies revealed that *Becn1* is involved in programmed cell death.[19–22] while the function of *Becn1* in HSCs has not yet been investigated.

In this study, we investigated the function of BECN1 in HSC maintenance by specifically knocking out *Becn1* in hematopoietic cells, and we observed that specific deficiency of *Becn1* resulted in disturbed homeostasis of the blood system and *Becn1* deficient HSCs displayed compromised reconstitution capacity by activating Caspase-3-GSDME signaling, but not through regulating autophagy. Together, this study elucidates the mechanism of BECN1 in modulating HSC function and raises an intriguing connection between BECN1 and GSDME-mediated pyroptosis. It serves as a reference for future research on how autophagy-related genes regulate stem cell function.

* *Address correspondence: Jianwei Wang, School of Pharmaceutical Sciences, Tsinghua University, Beijing 100084, China. E-mail address: jianweiwang@mail.tsinghua.edu.cn (Jianwei Wang).*

Conflicts of interest: The authors declare no conflicts of interest.

Author contributions: Conceptualization, J.W.W.; Methodology, X.X.Y.; Investigation, X.X.Y.; Writing – original draft, J.W.W.; Writing – review and editing, J.W.W., L.G.; Funding Acquisition, J.W.W.; Supervision, J.W.W.

Funding: This work was supported by grant numbers 2018YFA0800200, 2017YFA0104000, Z181100001818005 to J.W.W. from the National Key R&D Program of China or the Beijing Municipal Science & Technology Commission.

Supplementary Digital Content is available.

Blood Science, (2020) 2, 89-99

Received April 23, 2020; Accepted June 4, 2020.

http://dx.doi.org/10.1097/BS9.0000000000000051

2. RESULTS

2.1. *Becn1* deficiency results in a disturbed hematopoietic system

We crossed *Becn1*$^{flox/flox}$ mice with *Vav-iCre* mice and obtained the mice with the specific deficiency of *Becn1* in the blood system: *Becn1*$^{flox/flox}$*Vav-iCre* (hereafter named: *Becn1*^{vKO}). *Becn1*^{vKO} mice exhibited a significantly shorter lifespan compared to WT control mice in the same cohort (Fig. 1A). Moreover, there were more red blood cells (RBC) with a reduction of **mean corpuscular volume (MCV)** and an elevation of red blood cell distribution width (RDW-CV) in *Becn1*^{vKO} mice (Fig. 1B and C), but the amount of hemoglobin in *Becn1*^{vKO} mice decreased when it was compared with that in WT mice (Fig. 1C), indicating that *Becn1* deficiency results in microcytic hypochromic anemia even though it had enhanced erythropoiesis in *Becn1*^{vKO} mice. Meanwhile, the deficiency of *Becn1* affected the production of platelets (Fig. 1B). Next, we evaluated the lineage distribution in peripheral blood and bone marrow of *Becn1*^{vKO} mice and observed no difference in peripheral blood (Fig. 1D), but less myeloid cells in the bone marrow of *Becn1*^{vKO} mice compared to control mice (Fig. 1E).

Given that hematopoietic stem and progenitor cells (HSPCs) are the sources of all blood cells, we then investigated the HSPCs in bone marrow (gating strategy was shown in Sup. Fig. 1A, http://links.lww.com/BS/A10). The total cell number of bone marrow did not change (Sup. Fig. 1B, http://links.lww.com/BS/A10), while the percentage of hematopoietic stem cells (long-term HSC: LT-HSC), HSPCs (Lin$^-$/Sca-1$^+$/c-Kit$^+$: LSK) and common lymphoid progenitors (CLP) were decreased in *Becn1*^{vKO} mice (Fig. 1F and G), the percentage of megakaryocyte-erythroid progenitor (MEP) cells were increased and the percentage of other progenitors remained static (Fig. 1F and G). The increase of MEP cells was consistent with the increase of RBC in peripheral blood of *Becn1*^{vKO} mice (Fig. 1B and G). The number of LT-HSCs in *Becn1*^{vKO} mice was reduced, while the number of ST-HSCs (short-term HSCs) did not show any obvious change (Fig. 1H), indicating that the LT-HSC is disturbed by BECN1 loss.

Given that spleen is the primary site of stress erythropoiesis in mice with anemia,[23] and that splenomegaly is a typical sign of stress erythropoiesis,[23] we, therefore, investigated the spleen and found that spleens were significantly larger with an increase of weight from *Becn1*^{vKO} mice than those from control mice (Fig. 1I). Moreover, both the percentage and the absolute number of LT-HSC and MEP cells were increased in the spleen of *Becn1*^{vKO} mice, as well as the number of MPP cells and CMP cells (Fig. 1J and K). The increase of HSC and progenitor cells in the spleen of *Becn1*^{vKO} mice further suggested that *Becn1* dysfunction led to extramedullary hematopoiesis in the spleen. Consistently, the ratio and the absolute number of erythroid cells (Ter119$^+$) in the spleen of *Becn1*^{vKO} mice was increased (Sup. Fig. 1C and D, http://links.lww.com/BS/A10), which further indicated an enhancement of extramedullary hematopoiesis/erythropoiesis in the spleen.

2.2. *Becn1* deficiency impairs HSCs

Given that HSCs generate all blood cells throughout the lifespan, we then start to investigate the function of *Becn1* deficient HSCs. HSCs freshly isolated from *Becn1*^{vKO} mice were competitively transplanted into lethally irradiated recipient mice together with 2.5×10^5 competitor cells and the chimerism of peripheral blood of recipients was evaluated every 4 weeks until the 4th month (Fig. 2A). The result showed that the reconstitution capacity of *Becn1*^{vKO} HSCs was severely impaired (Fig. 2B), which was manifested by the reduction of all three lineages (Fig. 2B; gating strategy was shown in Sup. Fig. 2A, http://links.lww.com/BS/A11). The donor-derived lineage distribution in peripheral blood revealed that *Becn1* deficient HSCs display significantly differentiation bias towards T lineage and reduced myeloid potential at the end of the 4th month after transplantation (Fig. 2C; gating strategy was shown in Sup. Fig. 2B, http://links.lww.com/BS/A11). Moreover, analysis of the bone marrow of recipients revealed a striking decrease in the number of *Becn1*^{vKO}-derived HSCs and LSK cells (Fig. 2D and E; gating strategy was shown in Sup. Fig. 2C, http://links.lww.com/BS/A11), indicating that *Becn1* deficiency results in the loss of self-renewal capacity of HSCs.

The previous study revealed that loss of quiescence of HSCs resulted in the reduction of self-renewal capacity,[24,25] we then sought to investigate the cell cycle status of HSCs and found that *Becn1*^{vKO} HSCs were more active with an increased percentage at G_1 and $S/G_2/M$ stage but reduced percentage at G_0 stage (Fig. 2F and G), indicating that BECN1 might be a positive regulator of HSC quiescence.

The impairment of reconstitution and self-renewal ability of *Becn1*^{vKO}-derived HSCs along with the reduction of HSC cell number in the steady state indicates that BECN1 plays an important role in maintaining HSCs.

2.3. Dysfunction of BECN1 in HSPCs results in activated pyroptosis

BECN1 is a BH3-only protein,[18] and other BH3-containing proteins like Bid, Bad, Bim, Noxa, and PUMA play a role in programmed cell death,[26,27] and that damaged HSCs underwent apoptosis or repaired once entering cell cycle,[28,29] and that the frequency of HSCs in *Becn1*^{vKO} mice was significantly decreased (Fig. 1F), and that *Becn1* deficient HSCs lost quiescence (Fig. 2F), it is conceivable that *Becn1* deficient HSCs may suffer from the stress of programmed cell death or relevant pathway(s). To test this hypothesis, we seeded 8000 LSK cells isolated from WT and *Becn1*^{vKO} mice, and cell viability was evaluated 24 h later by **Fluorescence-activated cell sorting** (FACS). The result showed that the percentage of apoptotic cells, which was represented as Annexin V$^+$/PI$^-$, remained static between WT and *Becn1* deficient LSK cells (Fig. 3A and B), but the percentage of necrotic cells, which was represented as Annexin V$^+$/PI$^+$, was significantly higher in *Becn1* deficient LSK cells (Fig. 3A and B), the increase of necroptotic cell death in *Becn1* deficient LSK cells was also confirmed by DAPI uptake (Fig. 3C), suggesting that *Becn1* deficient HSPCs underwent cell death rapidly upon proliferation stress. To identify the gene(s) leading to the death of *Becn1* deficient HSPCs, we evaluated three classical cell death-related pathways, including apoptosis (wherein Caspase-3 is the main player[30]), necroptosis (wherein RIPK1-RIPK3-MLKL are the main players[31,32]) and pyroptosis (wherein GSDMD and GSDME are the main well studied players[33–35]). We conducted western blotting assays by using fresh *Becn1*^{vKO} and WT c-Kit$^+$ bone marrow cells to evaluate the expression of Caspase-3, RIPK3, MLKL, phosphorylated MLKL (hereafter named p-MLKL), GSDMD, and GSDME. The results revealed that RIPK3, MLKL, p-MLKL, and GSDMD remained static in *Becn1* deficient cells (Fig. 3D), indicating that RIPK3-MLKL-mediated necroptosis and GSDMD-mediated pyroptosis signaling is not activated in response to *Becn1* dysfunction in HSPCs. While, more Caspase-3 and GSDME were turn to the activated form, which was represented by cleaved-CASP3 and GSDME-N

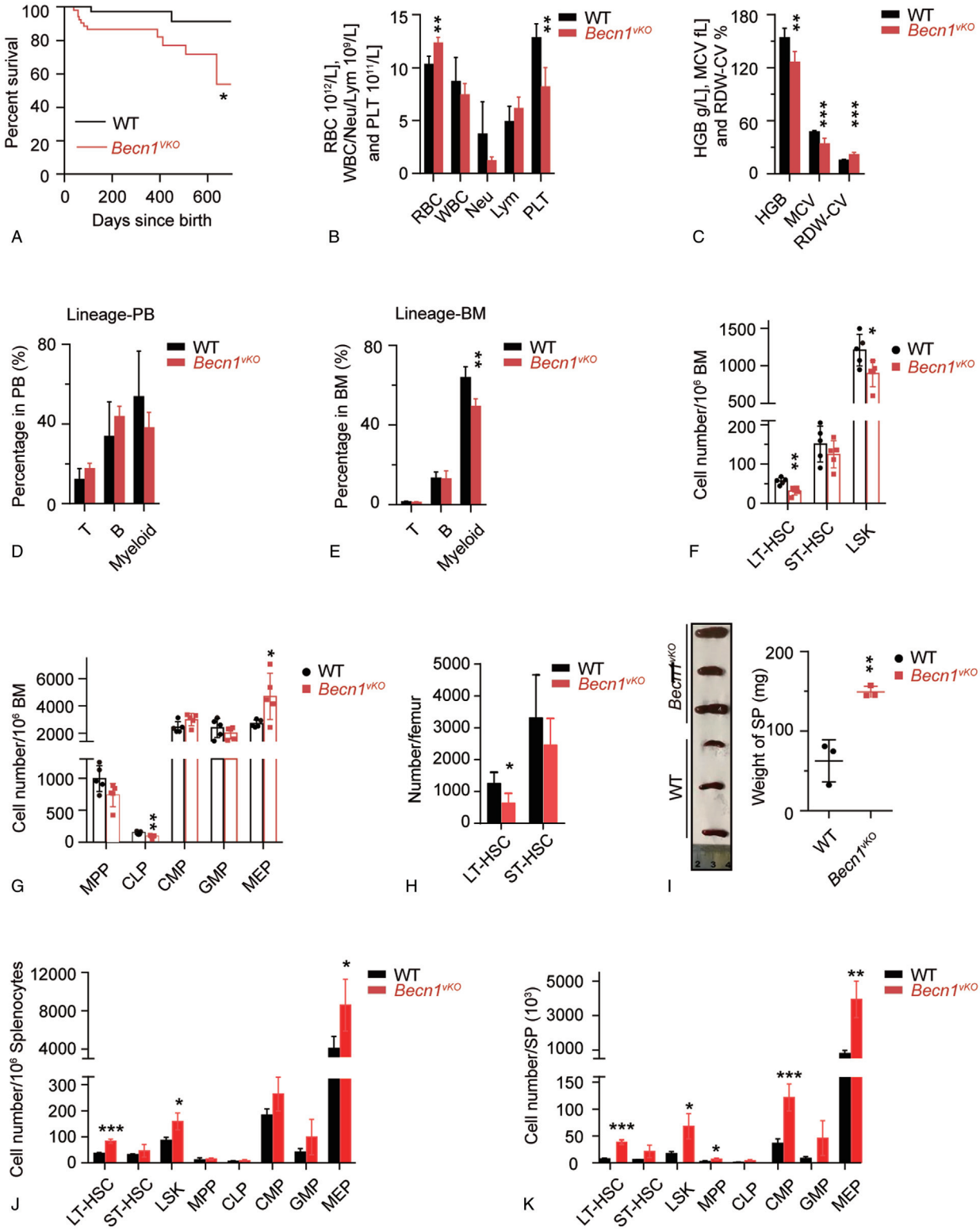

Figure 1. *Becn1* deficiency impairs homeostasis of the blood system. (A) Kaplan–Meier survival plot depicts survival curves for *Becn1*^{vKO} mice (n = 53) and WT mice (n = 37). (B and C) These histograms exhibit the complete blood cell counts of peripheral blood samples from WT and *Becn1*^{vKO} mice, including RBC (red blood cell), WBC (white blood cell), Neu (neutrophil), Lym (lymphoid cell), PLT (platelet) (B), HGB (hemoglobin), MCV (mean corpuscular volume), RDW (red cell distribution width) (C). Data are shown as mean ± SD, n = 5 mice per group. (D and E) This histogram shows the lineage distribution of peripheral blood (D) and bone marrow (E) for WT and *Becn1*^{vKO} mice, including T cells (CD3$^+$), B cells (B220$^+$), and myeloid cells (CD11b$^+$). Data are shown as mean ± SD, n = 5 mice per group. (F and G) The histograms display the number of HSPCs per million bone marrow cells of WT and *Becn1*^{vKO} mice, including LT-HSC (long term-HSC, CD34$^-$/Flt3$^-$LSK), ST-HSC (short term-HSC, CD34$^+$/Flt3$^-$LSK), LSK (Lin$^-$/Sca1$^+$/c-Kit$^+$) (F), MPP (multipotent progenitor, CD34$^+$/Flt3$^+$/LSK), CLP (common lymphoid progenitor, CD127$^+$/Flt3$^+$/LS^{low}K^{low}), CMP (common myeloid progenitor, Lin$^-$/Sca1$^-$/c-Kit$^+$/CD34$^+$/CD16/32^{low}), GMP (granulocyte/macrophage progenitor, Lin$^-$/c-Kit$^+$/Sca1$^-$/CD34$^+$/CD16/32^{high}) and MEP (megakaryocytic/erythroid progenitor, Lin$^-$/c-Kit$^+$/Sca1$^-$/CD34$^-$/CD16/32$^-$) (G) (n = 5 mice per group). Data are

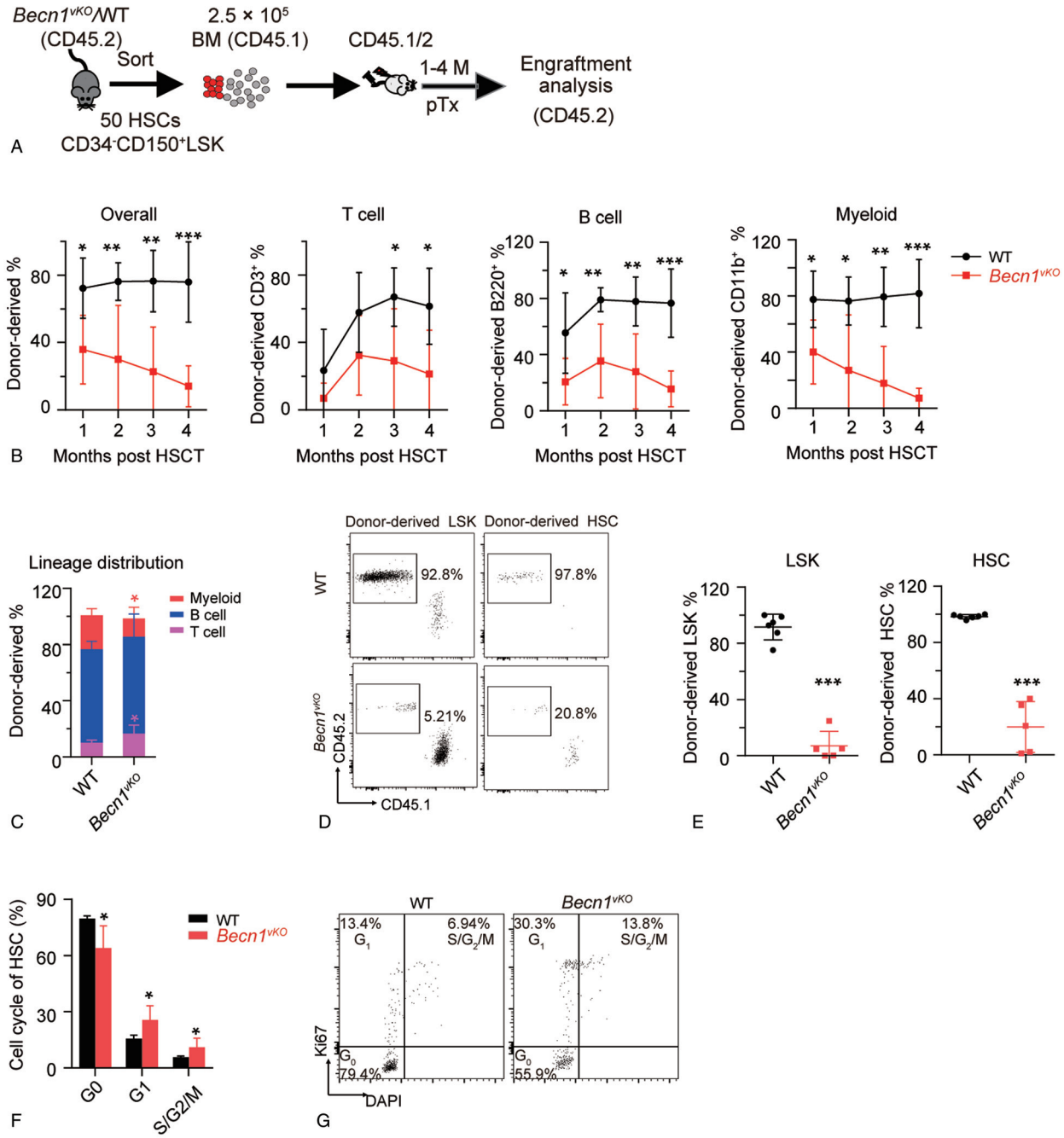

Figure 2. *Becn1* deficiency reduces HSC reconstitution. (A–C) Freshly isolated 50 HSCs from WT or *Becn1*^{vKO} mice were transplanted into lethally irradiated recipients together with 2.5×10^5 competitor cells. Chimerism in peripheral blood was evaluated every month until the fourth month post transplantation (Tx). (A) The schematic diagram showing the experimental design for HSC competitive transplantation. (B) The line plots showing donor chimerism in overall (CD45.2$^+$), T (CD3$^+$), B (B220$^+$) and myeloid (CD11b$^+$) cell every month after HSC transplantation (HSCT) (n = 6 for WT and 5 for *Becn1*^{vKO} group). The gating strategy to generate these line plots is presented in sup. Fig. 2A, http://links.lww.com/BS/A11. (C) This histogram displays the lineage distribution of donor-derived peripheral blood at the fourth month after transplantation (n = 6 for WT and 5 for *Becn1*^{vKO} group). Data are shown as mean ± SD. The gating strategy for lineage distribution is presented in sup. Fig. 2B, http://links.lww.com/BS/A11. (D and E) Representative flow cytometry plots (D) and scatter plot (E) showing donor-derived LSK and HSC engraftment in recipient bone marrow at the 4th month post-HSC transplantation (n = 6 for WT and 5 for *Becn1*^{vKO} group). Data are shown as mean ± SD. The gating strategy of LSK and HSC engraftment is presented in sup. Fig. 2C, http://links.lww.com/BS/A11. (F and G) The histogram (F) and representative flow cytometry plots (G) display the cell cycle analysis of WT and *Becn1*^{vKO} HSCs. n = 5 mice per group, data are shown as mean ± SD.

shown as mean ± SD. (H) The histogram displays the number of LT-HSC and ST-HSC per femur (n = 5 mice per group). Data are shown as mean ± SD. (I) This photograph (left) and scatter plot (right) exhibit the differences of spleens from WT and *Becn1*^{vKO} mice (n = 3 for each group). Data are shown as mean ± SD. (J and K) The histograms display the ratio (J) and absolute number (K) of HSPCs from spleens of WT and *Becn1*^{vKO} mice. Data are shown as mean ± SD, n = 3 mice for WT and 4 mice for *Becn1*^{vKO} group. The gating strategy of HSPCs is shown in sup. Fig. 1A, http://links.lww.com/BS/A10 1A for (F–H) and in sup. Fig. 1E, http://links.lww.com/BS/A10 for (J and K). Adult mice were analyzed at 4 to 5-month-old for (B–K).

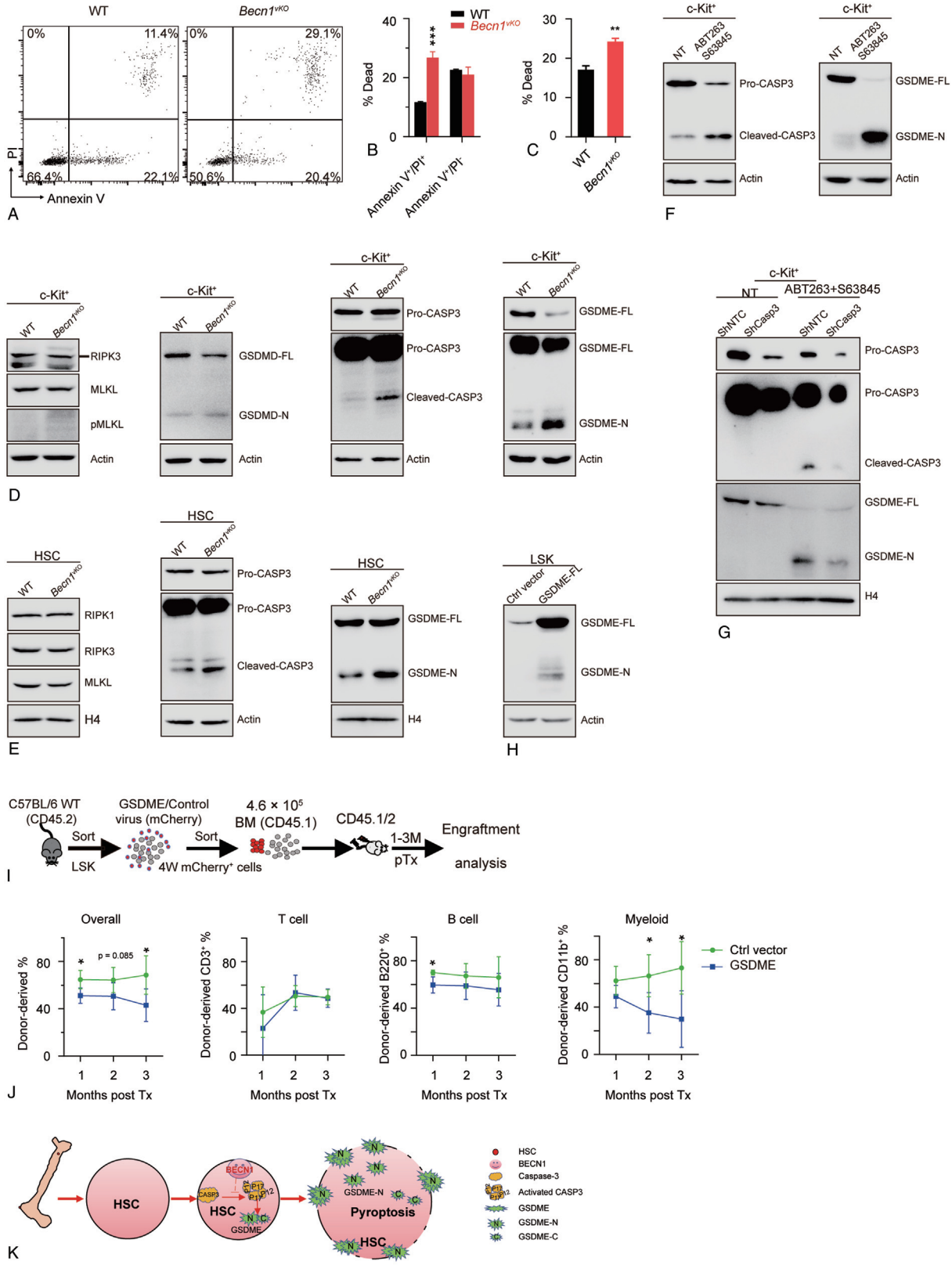

Figure 3. *Becn1* deficient HSCs show increased GSDME-mediated pyroptosis. (A–C) Representative flow cytometry plots (A) and histograms (B and C) showing cell viability of LSKs from WT and *Becn1*^{vKO} mice. Freshly isolated LSKs were cultured for 24 h before cell viability analysis by Annexin V (A and B) or DAPI (C). n = 3 repeats per group, data are shown as mean ± SD. (D) Representative western blot showing the level of RIPK3, MLKL, pMLKL, GSDMD, GSDME, and Caspase-3 (CASP3) in freshly isolated hematopoietic progenitor (c-Kit$^+$) cells from WT and *Becn1*^{vKO} mice. Cell lysates were subjected to immunoblot analysis using indicated antibodies. pMLKL, phosphorylated MLKL; GSDME-FL, full-length GSDME; GSDME-N, the N-terminal product of GSDME. (E) Representative western blot showing the level of RIPK3, MLKL, GSDME, and Caspase-3 in HSCs (CD34$^-$LSK) from WT and *Becn1*^{vKO} mice. Freshly isolated HSCs were cultured for 8 days. Cell lysates were subjected to immunoblot analysis using indicated antibodies. (F) Representative western blot showing the activation of Caspase-3 and GSDME

respectively (Fig. 3D), suggesting that apoptosis and GSDME-mediated pyroptosis might be activated in response to the loss of function of *Becn1*. To further verify this result in HSCs, we cultured 20,000 HSCs ($CD34^{-}LSK$) from WT and $Becn1^{\nu KO}$ mice in SFEM supplied with cytokine TPO and SCF for 8 days, and the protein levels of RIPK1, RIPK3, MLKL, Caspase-3, and GSDME were evaluated by western blotting. Consistently, proteins that mediated necroptosis in HSCs including RIPK1, RIPK3, and MLKL remained static while the activity of Caspase-3 and GSDME was elevated (Fig. 3E). These results suggest that *Becn1* deficiency leads to the activation of Caspase-3 and then the cleavage of GSDME, which furthermore results in the death of HSCs.

Our above results suggested that it was not the apoptotic cells, but the necrotic cells that increased significantly in *Becn1* deficient LSK cells (Fig. 3A–C), which indicating that apoptosis was not the main player, but another more "rapid" and necrotic cell death was caused in *Becn1* deficient HSPCs. Thus, although both Caspase-3 and GSDME were activated in *Becn1* deficient HSC and progenitors, the necrotic cell death should be eventually mediated by activated GSDME. A previous study reported that Caspase-3 cleaved GSDME to produce the N-terminal domain of GSDME (GSDME-N) and C-terminal domain of GSDME (GSDME-C), and that GSDME-N perforates membranes to induce a necrotic cell death which was called pyroptosis in GSDME-high-expressing cells and secondary necrosis/pyroptosis in GSDME-low-expressing cells.[34] Cells with high GSDME level underwent GSDME-mediated pyroptosis upon the activation of Caspase-3.[34] By exploring the database "ImmGen" and "BioGPS,"[36,37] we observed that the expression of GSDME in HSPCs is relatively high (Sup. Fig. 3A and B, http://links.lww.com/BS/A12), suggesting that the death of *Becn1* deficient LSKs may be due to the activation of Caspase3-GSDME-mediated pyroptosis. To test this hypothesis, WT $c\text{-}Kit^{+}$ bone marrow cells were treated with ABT263 and S63845 (both are apoptosis inducers[38,39]) for Caspase-3 activation, we observed the activation of Caspase-3 and interestingly, GSDME was cleaved to GSDME-N (Fig. 3F), indicating that GSDME-mediated pyroptosis was activated in response to the activation of Caspase-3. While when we knocked down Caspase-3 in $c\text{-}Kit^{+}$ cells, the cleaved GSDME-N was reduced compared to the control group (Fig. 3G), indicating that Caspase-3 lies upstream of GSDME and the activated Caspase-3 can cleave GSDME into GSDME-N. To further verify this hypothesis, first, we overexpressed the full-length mouse Caspase-3 in LSKs and transplanted them into recipient mice (Sup. Fig. 3C, http://links.lww.com/BS/A12), while they did not show any difference in either reconstitution or lineage differentiation after 3 months since the transplantation (Sup. Fig. 3D and E, http://links.lww.com/BS/A12). This may because the basal level of activated Caspase-3 was too low to leads to HSC cell death (Sup. Fig. 3F, http://links.lww.com/BS/A12). Since the N-terminal GSDME is the executor, then we cloned the N-terminal fragment of mouse GSDME (residues 1–270) into an overexpression lentiviral vector and tried to produce lentivirus carrying GSDME-N. Unfortunately, all 293T cells died of pyroptosis because of the toxicity of GSDME-N.[34,40] We then cloned the full-length cDNA of mouse GSDME and produced lentivirus overexpressing GSDME (GSDME-FL) (Fig. 3H), and transplanted the LSKs overexpressing GSDME into lethally irradiated recipient mice (Fig. 3I). Our result shows that the activation of GSDME-FL impairs the reconstitution capacity of HSCs (Fig. 3J).

Collectively, these results indicate that the dysfunction of *Becn1* in HSCs leads to the activation of Caspase-3 and then results in the cleavage of GSDME, and finally brings about the activation of pyroptosis and loss of function of HSCs (Fig. 3K).

2.4. BECN1 is dispensable in maintaining HSCs autophagy

Several studies reported that *Becn1* was a core gene involved in the early stage of autophagy,[19,41,42] while some other studies reported that BECN1 was dispensable in autophagy.[43–47] Previous studies showed that the lifespan of mice with specific deficiency of *Atg5* or *Atg7* in the blood system was <3 months,[13,14] and our result displays that the lifespan of $Becn1^{\nu KO}$ is shorter than WT controls but is still longer than *Atg5* or *Atg7* deficient mice (Fig. 1A). Moreover, $Becn1^{\nu KO}$ mice display relatively balanced lineage distribution in peripheral blood under steady-state (Fig. 1D), while *Atg7* or *Atg12* deficient mice specifically in the blood system exhibited a myeloid differentiation bias.[8] These differences imply that *Becn1* may play a distinguishing role in the blood system from other typical autophagy genes.

To explore whether the autophagy activity in HSCs is dependent on BECN1, we evaluated the autophagic flux of $c\text{-}Kit^{+}$ cells from WT and $Becn1^{\nu KO}$ mice by measuring the conversion ratio of LC3-II using western blot, wherein LC3-II accumulates significantly upon chloroquine treatment, which is a lysosome inhibitor, and the relative ratio of LC3-II to the loading controls such as actin between chloroquine treated and none treated group represents the autophagy flux of a sample.[48,49] We then treated $c\text{-}Kit^{+}$ bone marrow cells of WT and $Becn1^{\nu KO}$ mice with chloroquine and the transition of LC3-II was evaluated 4 h later. The result displayed that the transition of LC3-II was not reduced in $Becn1^{\nu KO}$ $c\text{-}Kit^{+}$ cells compared to WT control (Fig. 4A). To further test the above result, we measured the autophagic activity of LSK cells from WT and $Becn1^{\nu KO}$ mice by using Cyto-ID dye, which was an amphiphilic tracer and a relative specific dye to detect autophagy level in live cells.[50,51] This method was first validated on BM cells treated with the autophagy inducer rapamycin as well as the autophagy inhibitor chloroquine (Sup. Fig. 4A, http://links.lww.com/BS/A13), while the result on LSKs suggested that the transient autophagic level showed no difference between WT and $Becn1^{\nu KO}$ LSKs (Fig. 4B). To detect the autophagic degradation activity, LSKs were subjected to chloroquine and the autophagic flux was

following apoptotic drug treatment. WT $c\text{-}Kit^{+}$ cells were treated with ABT263 (10 μM) plus S63845 (10 μM) or mock treated for 5 h. Cell lysates were subjected to immunoblot analysis using indicated antibodies. (G) Representative western blot showing the level of Caspase-3 and GSDME in Caspase-3-shRNA or none target control (NTC) shRNA infected $c\text{-}Kit^{+}$ cells with or without apoptosis induction. WT $c\text{-}Kit^{+}$ cells were infected with lentivirus carrying an NTC shRNA or a Caspase-3-shRNA for 3 days and then treated with ABT263 (10 μM) plus S63845 (10 μM) or mock treated for 5 h. The infection rate was around 90% and the total cell population was collected for western blot analysis without further isolation. Cell lysates were subjected to immunoblot using indicated antibodies. (H) Representative western blot showing GSDME overexpression in LSKs. Freshly isolated 10^5 LSKs were infected with the full-length GSDME-cDNA or control vector for 3 days. Cell lysates of the total cell population were subjected to western blot using indicated antibodies. (I and J) 40,000 $mCherry^{+}$ cells were isolated from full-length GSDME-cDNA or control vector infected LSKs at 3 days post infection and transplanted into lethally irradiated recipients together with 4.6×10^5 competitor cells. Chimera in peripheral blood was evaluated every month until the third month. (I) The schematic diagram showing the experimental design for GSDME (full-length) overexpression transplantation. (J) The line plots depict changes in peripheral blood chimerism of donor-derived cells (CD45.2) in recipients at the indicated time points after transplantation. Data are shown as mean ± SD, n = 5 mice per group. (K) Model for regulation of BECN1 in HSCs cell death.

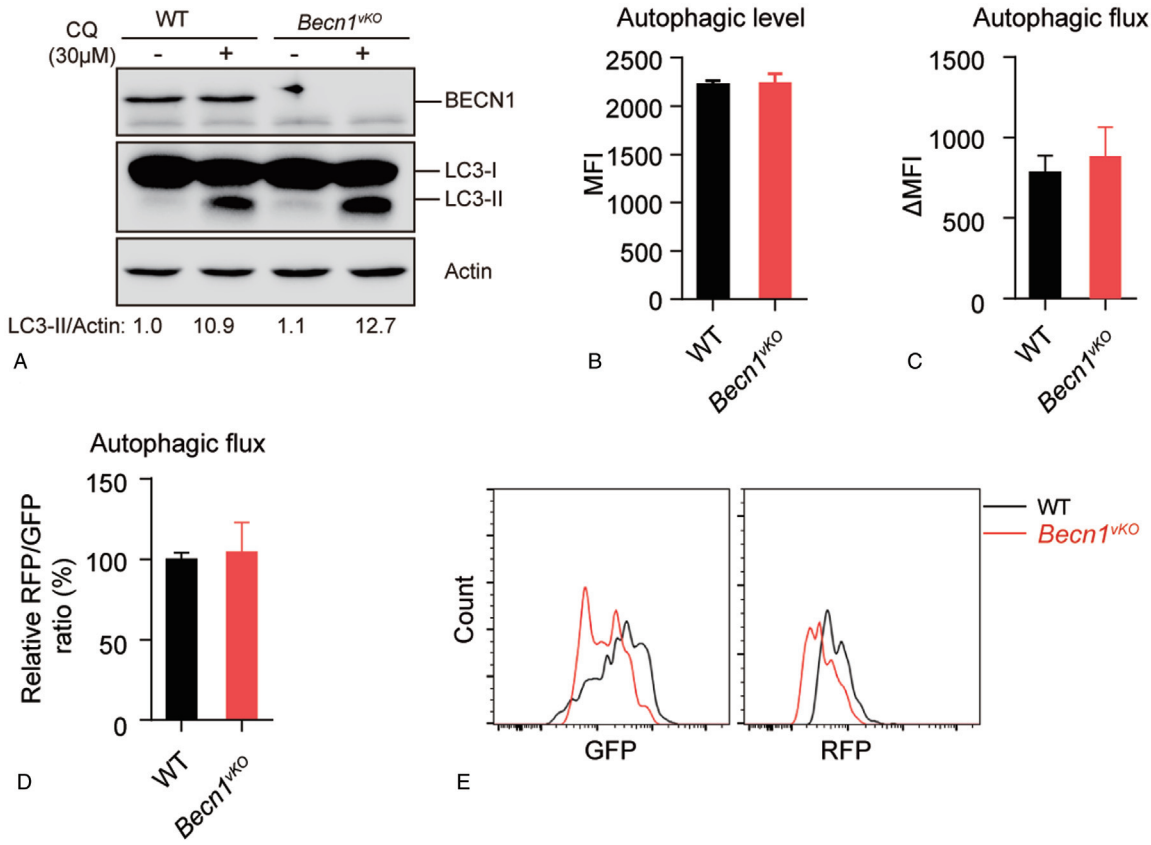

Figure 4. *Becn1* deficiency does not reduce the autophagy ability of HSCs. (A) Representative western blot showing LC3-II transition in c-Kit$^+$ cells from *Becn1*^{vKO} and WT control. 100,000 c-Kit$^+$ cells were treated with 30 μM chloroquine (CQ) or mock treatment for 4 h. Cell lysates were subjected to immunoblot using indicated antibodies. The intensity of the protein signal was measured by Image J. (B and C) The histograms show the transient autophagic level (MFI) (B) and autophagic flux (ΔMFI) (C) of LSKs from WT and *Becn1*^{vKO} mice by using Cyto-ID dye. 7500 freshly isolated LSKs were cultured for 24 h (B), and 9000 freshly isolated LSKs were cultured for 3 h before 15 μM chloroquine or mock treatment for another 21 h (C). Samples were stained with Cyto-ID dye and analyzed the fluorescence intensity of GFP by flow cytometry. ΔMFI was calculated as what was mentioned in the methods. n = 3 repeats per group, data are shown as mean ± SD. (D and E) The histograms display autophagic flux (D) and relative fluorescence intensity of RFP to GFP (E) of HSCs (CD48$^-$SK) from WT and *Becn1*^{vKO} mice by GFP-LC3-RFP-LC3ΔG plasmid. 10,000 fresh isolated LSKs form WT and *Becn1*^{vKO} mice were infected with GFP-LC3-RFP-LC3ΔG plasmid for 3 days, and then stained with the surface marker of HSC (CD48, Sca-1, c-Kit) before analyzing the GFP and RFP fluorescence intensity by flow cytometry. The autophagic flux was indicated by the relative fluorescence intensity of RFP to GFP and normalized to the WT group. n = 3 repeats per group, data are shown as mean ± SD for (D). The strategy to calculate the autophagic flux by using GFP-LC3-RFP-LC3ΔG plasmid is presented in sup. Fig. 4C, http://links.lww.com/BS/A13.

measured. Consistently, the autophagic flux did not change in *Becn1* deficient LKSs (Fig. 4C).

A recent study developed a sensitive approach to measure autophagy flux in primary cells.[52] In this system, GFP-LC3-RFP-LC3ΔG protein can be cleaved into GFP-LC3 and RFP-LC3ΔG fragments, in which GFP-LC3 can participate and be degraded in normal autophagy process, but RFP-LC3ΔG stays in the cytosol as a relatively stable internal control, thus the mean fluorescence intensity (MFI) of RFP to GFP ratio represents the autophagic flux.[52] We produced lentivirus expressing GFP-LC3-RFP-LC3ΔG and infected target cells for autophagic flux measurement. First of all, we validate the sensitivity of this approach on 293T and EL4 cells by rapamycin treatment (Sup. Fig. 4B, http://links.lww.com/BS/A13). Then we infected WT and *Becn1*^{vKO} LSK cells. Three days later, the autophagic flux was measured by FACS and the result shows that no difference was observed between WT and *Becn1* deficient HSCs (CD48$^-$ c-Kit$^+$ Sca-1$^+$) (Fig. 4D and E, the calculation method was shown in Sup. Fig. 4C, http://links.lww.com/BS/A13).

Taken together, our study shows that *Becn1* modulates the function of HSCs through Caspase-3-GSDME signaling, but not autophagy. Loss of BECN1 in HSCs leads to the activation of GSDME-mediated pyroptosis which directly results in HSC death and finally results in HSC dysfunction. Our study uncovered that BECN1 maintains HSC by acting as a negative regulator of GSDME-mediated pyroptosis.

3. DISCUSSION

Although *Becn1* is a classic gene in the field of autophagy, its role in autophagy is controversial. Some studies have reported that *Becn1* is necessary for autophagy,[53,54] but different studies were showing that some specific substances, such as cis-unsaturated,[46] arsenic trioxide, and resveratrol,[44,55] were able to induce autophagy in *Becn1* dysfunctional cells. In this study, we investigated the role of *Becn1* in HSC maintenance and found that targeted deletion of *Becn1* impaired HSCs by activating CASP3-GSDME-mediated pyroptosis, but not through autophagy. In addition to direct evidence supporting this conclusion (Fig. 4A–D), two previous reports revealed that the lifespan of mice with targeted deletion of *Atg5* or *Atg7* in the blood system was only about 3 months.[13,14] However, our data shows that the lifespan of hematopoietic-specific deletion of *Becn1* mice is much longer (Fig. 1A). These data may suggest that *Becn1* plays a role

in the blood system different from that of other canonical autophagy genes such as *Atg5* and *Atg7*.

Moreover, we observed that *Becn1* deficient HSCs lost quiescence, and underwent GSDME-mediated pyroptosis. The possible explanation could be that *Becn1* deficient HSCs are activated to replenish the loss caused by pyroptosis, eventually leading to the disturbed homeostasis of the blood system (Fig. 1B–K). Both CASP3 and GSDME were activated in *Becn1* deficient HSPCs (Fig. 3D and E), but pyroptosis rather than apoptosis was activated (Fig. 3A–C). The possible reason is that HSC's characteristics determine the occurrence of pyroptosis rather than apoptosis in response to *Becn1* dysfunction. HSCs are at a low metabolic state and mainly rely on glycolysis for energy supply, [1,56] which is a quick but inefficient manner even though it can offer a survival advantage under hypoxic conditions.[56,57] Activated HSCs increase the demands for ATP and further decrease their ATP level.[58] Apoptosis is a form of well-programmed cell death by forming apoptotic bodies, and it requires energy to complete this progress.[59,60] GSDME-mediated pyroptosis is a kind of necrosis,[34] and might demand little or no energy. Earlier studies showed that cells with a high ATP level died of apoptosis while necrosis with ATP depletion,[61] thus it is the ATP level inside a cell that matters for cell death decision. Therefore, damaged HSCs with low energy inside would prefer to die in an energy-saving way. Since more HSCs are activated and enter cell cycle upon BECN1 loss, which increases the ATP demands and decreases the internal ATP level of HSCs, these damaged and activated HSCs would probably prefer to die of necrosis under the proliferation stress since the energy shortage. GSDME-mediated pyroptosis might fit better for *Becn1* deficient HSCs than apoptosis in terms of energy. A previous study has shown that cells with a high GSDME level underwent pyroptosis but not apoptosis after chemotherapy drug treatment since pyroptosis was "faster" than apoptosis,[34] which correlated well with our discovery on the death mode preference. This death preference might also be controlled by cell energy levels inside.

Pyroptosis is a kind of lytic cell death and can release immunogenic cell contents,[31,40] including damage-associated molecular patterns (DAMPs), which could prevent the malignant transformation of HSCs. Both BECN1 and GSDME are reported tumor suppressors.[53,62]*Becn1* heterozygous mice show an increased incidence of lymphomas, lung, and liver cancers,[53,63] and 40% to 75% of prostate, breast, and ovarian cancers bear with monoallelic deletion of *Becn1*.[64]*Gsdme* silencing was found in cancers of the breast,[64] gastro,[65] and colorectum.[66] The loss of function of *Becn1* alone in HSC might be tumorigenic. To avoid tumor, GSDME-mediated pyroptosis was activated in *Becn1* deficient HSCs and led to rapid cell death with the release of DAMPs. Thus, the activation of GSDME-mediated pyroptosis may be a tissue-protective mechanism used by HSPCs to prevent malignancy after *Becn1* loss. This hypothesis may also be true for other tissues, for example, the prostate or breast does not express GSDME,[67] while tumor in these tissues are highly associated with *Becn1* monoallelic deletion.[63]

While there are some limitations to this study. First, autophagy is sensitive to environmental stimulation, since the technique limitation, we could not detect autophagy activity of fresh HSC in a relatively short time from mice, even by using the most sensitive method in measuring basal autophagic activity at present.[52] The transgenic mice expressing GFP-LC3-RFP-LC3ΔG combined with other HSC-specific reporter mice are necessary to be done to settle this problem. Second, since the low percentage of cells suffering from pyroptosis at one time, we could not provide a photograph to see the HSCs form $Becn1^{vKO}$ mice undergoing pyroptosis directly. Third, we only showed loss of function of HSCs with more GSDME activation, the detailed mechanism of GSDME-mediated pyroptosis pathway in HSC modulation needs to be studied further. Finally, as a well-studied autophagic related gene, we have only focused on the autophagic roles of BECN1, while its functions in the endocytic process of HSC is worth studying further.

In conclusion, our study raises the connection between GSDME-mediated pyroptosis and HSCs cell fate modulation, which gives us a new sight for understanding *Becn1* in the homeostasis of the blood system. While how does the GSDME pathway modulate HSC cell fate in detail, and whether is activated Caspase-3 the only proteinase to cleave and activate GSDME upon BECN1 loss? How does *Becn1* deficiency lead to Caspase-3 activation and GSDME-mediated pyroptosis? Is it shared by other autophagy genes or *Becn1*-specific? These questions need to be studied further. The non-canonical autophagy machinery and its physiological function are also worth discussion in future investigation.

4. MATERIALS AND METHODS

4.1. Animals

$Becn1^{flox/flox}$ (CD45.2, #028794), *Vav-iCre* (CD45.2), C57BL/6 (CD45.2), C57BL/6-SJL (CD45.1), and CD45.1/2 mice. $Becn1^{flox/flox}$ mice were purchased from Jackson Laboratory and were crossed with *Vav-iCre* mice to obtain *Becn1* specific deleted mice in the blood system. CD45.1/2 mice were obtained by crossing CD45.1 and CD45.2 mice. Mice were all C57BL/6 background and maintained in specific pathogen-free (SPF) animal facility. Mice of both genders were used and all experiments were approved by the Institutional Animal Care and Use Committee (IACUC) of Tsinghua University.

4.2. Antibodies for flow cytometry

The fluorescence conjugated antibodies were used for flow cytometry: anti-c-Kit-APC (1:100, eBioscience, 17–1171–82), anti-APC-microbeads (1:50, Miltenyi Biotec, 130–090–855), Streptavidin-APC-Cy7 (1:100, BioLegend, 405208), Streptavidin-PerCP-Cy5.5 (1:100, BD Biosciences, 551419), anti-Sca-1-PE-Cy7 (1:100, BD Biosciences, 558162), anti-CD150-PE (1:100, BioLegend, 115904), anti-CD150-Brilliant Violet 605 (1:100, BioLegend, 115927), anti-CD34-FITC (1:25, eBioscience, 11–0341–81), anti-CD34-AF700(1:25, eBioscience, 56–0341–82), anti-Flt3-PE-CF594 (1:100, BD Biosciences, 562537), anti-CD16/32-FITC (1:100, eBioscience, 11–0161–85), anti-CD127-Brilliant Violet 421 (1:100, BioLegend, 135024), anti-CD48-PerCP-Cy5.5 (1:100, BioLegend, 103422), anti-CD3-APC (1:300, BioLegend, 100312), CD4-PerCP-Cy5.5 (1:300, BioLegend, 100434), anti-CD8-FITC (1:300, BioLegend, 100706), anti-B220-V500 (1:300, BD Biosciences, 561226), anti-B220-FITC (1:300, BioLegend, 103206), anti-B220-Alexa Fluor 700 (1:300, BioLegend, 103232), anti-B220-PB (1:700, Biolegend, 103227), anti-CD11b-PerCP-Cy5.5 (1:300, BioLegend, 101228), anti-CD11b-APC-eFluor780 (1:300, eBioscience, 47-0112-82), anti-CD11b-PE-Cy7 (1:300, BioLegend, 101216), anti-Ter119-FITC (1:250, BioLegend, 116215) anti-CD45.1-FITC (1:300, BioLegend, 110706), anti-CD45.1-Alexa Fluor 700 (1:300, BD Biosciences, 561235), anti-CD45.2-PE (1:300, BioLegend, 109808) and anti-CD45.2-FITC (1:300, BioLegend, 109806). The biotin labeled lineage antibodies were from BioLegend: anti-Ter-119 (116204), anti-CD3 (100244), anti-CD4 (100508), anti-CD8 (100704), anti-B220 (103204), anti-CD11b (101204), and anti-Gr-1 (108404).

4.3. Complete blood cell counts

Peripheral blood samples were obtained from the tail using EDTA-containing tubes and performed by an automatic hematology analyzer BC-5000 (Mindary).

4.4. Cell sorting and flow cytometry

Bone marrow cells were isolated by crushing tibia, femur and pelvic bones (with spines for some experiments) in D-HANK'S buffered saline solution containing 2% fetal bovine serum (FBS), 1% HEPES and 50 U/mL penicillin/streptomycin (HBSS+), and filtered through100 μm nylon strainer. For hematopoietic stem and progenitor (c-Kit$^+$) cells enrichment, bone marrow cells were stained with c-Kit-APC followed by anti-APC-microbeads and MACS Separation LS Columns from Miltenyi Biotec. For HSC sorting, c-Kit$^+$ cells were stained with Streptavidin-APC-Cy7, Sca-1-PE-Cy7, c-Kit-APC, CD150-PE, CD34-FITC following the biotin-labeled lineage antibodies against Ter-119, CD3, CD4, CD8, B220, CD11b, and Gr-1. For LSK cells sorting, c-Kit$^+$ cells were stained with Streptavidin-APC-Cy7, Sca-1-PE-Cy7, and c-Kit-APC following the biotin-labeled lineage antibodies. Cells were stained with 10 ng/mL DAPI before cell sorting by Influx/FACS Aria SORP (BD Biosciences). DAPI negative population was sorted as living cells.

For HSC and progenitor analysis, 1×10^7 femur-derived bone marrow cells or splenocytes were stained with Sca-1-PE-Cy7, c-Kit-APC, CD34-AF700, Flt3-PE-CF594, CD16/32-FITC, CD127- Brilliant Violet 421, and Streptavidin-APC-Cy7 following the biotin-labeled lineage antibodies mentioned above. Cells number was measured by a Vi-CELL XR cell viability analyzer (Beckman Coulter). For lineage analysis, samples from peripheral blood and bone marrow were stained with CD3-APC, B220-FITC, and CD11b-PerCP-Cy5.5, splenocytes were stained with Ter119-FITC. Tail-derived peripheral blood samples by using EDTA-containing tubes were lysed with ACK lysis buffer. Bone marrow cells were from femur and splenocytes were dissociated by slides. For peripheral blood chimerism analyses, cells were stained with CD3-APC, B220-Alexa Fluor 700, CD11b-PerCP-Cy5.5, together with CD45.1-FITC and CD45.2-PE for HSCs transplantation, and CD3-APC, B220-PB, CD11b-APC-eFluor780, together with CD45.1-Alexa Fluor 700 and CD45.2-FITC (CD45.1/2 recipients) or CD45.1-FITC (CD45.2 recipients) for gene overexpression transplantation. For HSC chimerism analyses, femur-derived bone marrow cells from recipients were stained with Streptavidin-PerCP-Cy5.5, Sca-1-PE-Cy7, c-Kit-APC, CD150-Brilliant Violet 605 and CD34-Alexa Fluor 700 together with CD45.1-PE and CD45.2-FITC after biotin-labeled lineage antibodies mentioned above. The cells were performed on Fortessa (LSR Fortessa, BD Biosciences).

4.5. Transplantation

For HSCs transplantation, 50 HSCs (CD45.2) were freshly isolated and injected into lethal irradiated (10 Gy, delivered in two doses 3 h apart) recipient mice (CD45.1/2) from the tail vein with 2.5×10^5 CD45.1-derived total bone marrow cells as competitors. The lethal radiation was taken using an X-ray irradiator (RS 2000, Rad Source Technologies). For over-expression experiment, LSKs were isolated from lower libs and spines of WT CD45.2 mice, 10^5 LSKs were plated per well in 96-well plate and infected with cDNA or control vector for 3 days, mCherry$^+$ cells were isolated and transplanted into lethally irradiated recipients with CD45.1-derived total bone marrow cells as the competitor. The lineage tracking of peripheral blood was taken every month post-transplantation till the 4th month for HSCs transplantation and 3rd month for vector infected transplantation. The HSCs and LSKs chimerism were analyzed at the 4th month. The antibodies used to analyze the chimerism of peripheral blood and bone marrow were listed above.

4.6. In vitro cell culture and apoptosis induction

293T cells were maintained in Dulbecco's modified Eagle's medium (DMEM), and EL4 cells were cultured in RPMI 1640 medium, supplied with 10% FBS. Primary hematopoietic cells were cultured in StemSpan serum-free medium (SFEM) (Stem Cell Technologies, #09650, Vancouver, Canada) supplied with 20 ng/mL mTPO (Peprotech, 315–14), 20 ng/mL mSCF (Peprotech, 250–03) and 50 U/mL penicillin/streptomycin (Hyclone, SV30010). All cells were cultured at 37°C with 5% CO_2. For apoptosis induction, 2×10^6 c-Kit$^+$ cells were treated with 10 μM ABT263 (Selleck, S1001) and 10 μM S63845 (Selleck, S8383) for 5 h before western blot procedure mentioned above.

4.7. Cell cycle and cell viability assay

For HSC cell cycle analysis, 3×10^6 c-Kit$^+$ cells were enriched and stained with relative surface markers, then fixed for 15 min, washed and permed along with intracellular Ki67 staining for 30 min by using FIX and PERM® Cell Fixation & Permeabilization Kit (Invitrogenused, GAS004) and Ki67-FITC (BD Biosciences, 558616), then stained with 50 μg/mL DAPI (Sigma, D8417). For cell viability assay, 8000 LSKs were plated per well and cultured in SFEM for 24 h, then washed and stained with-Annexin V-FITC (BD Biosciences, 556420) and Propidium iodide (MCE, #HY-D0815/CS-7538) according to the product introduction, DAPI (20 ng/mL) uptake was performed on LSKs after 24-h cultivation at an initial number of 2000 to 3000.

4.8. Western blot analysis and related antibodies

Fresh isolated c-Kit$^+$ cells were lysed with NETN buffer (0.5% Nonidet P-40, 1 mM EDTA, 20 mM Tris–HCl, pH 8.0, 100 mM NaCl, containing protease and phosphatase inhibitors cocktail) for 30 min on ice, then centrifuged at 13,000 rcf for 10 min, 4°C. The supernatant was collected and boiled with 1 × SDS loading (4% SDS, 50 mM Tris base pH6.8, 20% glycerol, 04% Bromphenolblau) at 100°C for 8 min. In vitro cultured c-Kit$^+$ cells, LSKs and HSCs were collected and sonicated by Sonicator (Diagenode, Bioruptor plus) in 1 × SDS loading and then boiled before running the SDS-PSGE according to the regular procedure for western blot. Samples were subjected to 13.5% or 15% SDS-PAGE with rabbit-derived primary antibodies against Caspase-3 (1:800, CST, 9662S) and LC3 (1:3000, Sigma, L7543), 10% SDS-PAGE with antibodies against RIPK3 (1:1000, PROSCI, 2283), MLKL (1:1000, ANGENT, AP14272b), Phospho-MLKL (1:1000, Abcom, ab196436), GSDMD (1:1000, Abcam, ab209845), GSDME (1:1000, Abcam, ab215191) and BECN1 (1:700, Proteintech, 11306–1-AP). H4 (1:1000, Proteintech, 16047–1-AP) and Actin (1:1000, HuaBio, ET1701–80) were used as the internal reference. HRP-linked anti-rabbit IgG (1:10,000, Cell Signalling, 7074S) was used as the secondary antibody.

4.9. Plasmid construction and lentivirus packaging

Mouse cDNA for full-length GSDME (forward primer: GACAGACTAGTTCGACGCGTATGTTTGCCAAAGCAACT-CG and reverse primer: GGGAGGGAGAGGGGCGGATCCC-TAGTCTTGACCTGTAGCAT), N-terminal GSDME (the same forward primer as full-length GSDME and reverse primer: GGGAGGGAGAGGGGCGGATCCCTAATCCAGCATGTCC-AGAAAGG), and full-length Caspase-3 (forward primer:

GACAGACTAGTTCGACGCGTGCCACCATGGAGAACAA-CAAAACCTCAGTG and reverse primer: GGGAGGGAGA-GGGGCGGATCCCTAGTGATAAAAGTACAGTTCTTTCGT-G) were amplified and inserted into an overexpression vector pRRL-cDNA-IRES2-mCherry, modified from pRRL-PPT-SF-newMCS-IRES2-EGFP by replacing EGFP by mCherry. shRNA targeted Caspase-3 was cloned into SF-LV-miRE-EGFP plasmid with the target sequence: TGCTGTTGACAGTGAGCGCCA-CGAAAGAACTGTACTTTTATAGTGAAGCCACAGATGTA-TAAAAGTACAGTTCTTTCGTGATGCCTACTGCCTCGA. The high-fidelity DNA polymerase (Vazyme, P515–02) and homologous recombination kit (TIANGEN, V1201–01) were used for plasmid construction. 293T cells were transfected with 16 μg core plasmid along with two helper plasmids psPAX2 and pMD2.G using Polyethylenimine (Polysciences, 23966). The medium was collected at 48 and 72 h and concentrated using ultracentrifuge (Beckman, OPTIMA XE-90), as previously described.[68]

4.10. Autophagic activity measurement

For autophagic activity measurement by western blot, 10^5 c-Kit$^+$ cells were cultured overnight in SFEM medium and treated with or without 30 μM chloroquine for 4 h, samples were sonicated and boiled in 1 × SDS loading. The autophagic activity of the sample was compared by the LC3-II/actin ratio between the chloroquine treated and none treated group. By using Cyto-ID dye (1:2000, Enzo, ENZ-51031-0050), 7500–9000 LSKs were plate per well cultured for 24 h, three duplicates were prepared, then washed with HBSS+ buffer and stained with Cyto-ID dye for 20 min at cell culture condition, then washed and resuspended in HBSS+ buffer containing 10 ng/mL DAPI and analyzed by flow cytometry. The transient autophagic level was indicated by MFI. For autophagic flux measurement, freshly isolated LSKs were cultured for 3 h and then were incubated with or without 15 μM chloroquine for another 21 h. Autophagic flux was indicated by the increase of MFI (ΔMFI) between chloroquine treated and none treated group: ΔMFI Cyto-ID = MFI Cyto-ID (+CQ) − MFI Cyto-ID (−CQ). By using GFP-LC3-RFP-LC3ΔG plasmid, lentiviruses were prepared and infected 10,000 LSKs, 3 duplicates were prepared and stained for Sca-1-PE-Cy7, c-Kit-APC, and CD48-PerCP-Cy5.5 before flow cytometry analysis. Autophagic flux was indicated by the relative ratio of MFI (RFP) to MFI (GFP), finally, the ratio was normalized to the WT group. For Cyto-ID method verification, BM cells were treated with 300 nM rapamycin and 15 μM chloroquine for 18 h before flow cytometry analysis. For GFP-LC3-RFP-LC3ΔG plasmid verification, GFP and RFP double-positive 293T and EL4 cells were isolated after lentivirus infection and treated with 300 nM Rapamycin for 13 h before flow cytometry analysis.

4.11. Statistics

All data are presented as mean ± standard deviation (SD). Statistical significance was determined using a two-tailed unpaired Student's *t* test by GraphPad Prism 6.0 and was considered significant when ≤ 0.05. * $P \leq .05$, ** $P \leq .01$, *** $P \leq .001$; ns, not significant. The survival curve is analyzed using the log-rank test. All experiments were repeated twice or more times independently.

ACKNOWLEDGMENTS

We thank Dr. Axel Schambach for the kind gift of the pRRL-PPT-SF-newMCS-IRES2-EGFP vector.

REFERENCES

[1] Kohli L, Passegue E. Surviving change: the metabolic journey of hematopoietic stem cells. *Trends Cell Biol* 2014;24(8):479–487.
[2] Mohyeldin A, Garzon-Muvdi T, Quinones-Hinojosa A. Oxygen in stem cell biology: a critical component of the stem cell niche. *Cell Stem Cell* 2010;7(2):150–161.
[3] Parmar K, Mauch P, Vergilio JA, Sackstein R, Down JD. Distribution of hematopoietic stem cells in the bone marrow according to regional hypoxia. *PNAS* 2007;104(13):5431–5436.
[4] Acar M, Kocherlakota KS, Murphy MM, et al. Deep imaging of bone marrow shows non-dividing stem cells are mainly perisinusoidal. *Nature* 2015;526(7571):126–130.
[5] Spencer JA, Ferraro F, Roussakis E, et al. Direct measurement of local oxygen concentration in the bone marrow of live animals. *Nature* 2014;508(7495):269–273.
[6] Toshio Suda M, Arai F, Shimmura S. Regulation of stem cells in the niche. *Cornea* 2005;24:S12–S17.
[7] Takubo K, Nagamatsu G, Kobayashi CI, et al. Regulation of glycolysis by Pdk functions as a metabolic checkpoint for cell cycle quiescence in hematopoietic stem cells. *Cell Stem Cell* 2013;12(1):49–61.
[8] Ho TT, Warr MR, Adelman ER, et al. Autophagy maintains the metabolism and function of young and old stem cells. *Nature* 2017;543 (7644):205–210.
[9] Marino G, Pietrocola F, Eisenberg T, et al. Regulation of autophagy by cytosolic acetyl-coenzyme A. *Mol Cell* 2014;53(5):710–725.
[10] Dikic I, Elazar Z. Mechanism and medical implications of mammalian autophagy. *Nat Rev Mol Cell Biol* 2018;19(6):349–364.
[11] Levine B, Kroemer G. Biological functions of autophagy genes: a disease perspective. *Cell* 2019;176(1–2):11–42.
[12] Liu F, Lee JY, Wei H, et al. FIP200 is required for the cell-autonomous maintenance of fetal hematopoietic stem cells. *Blood* 2010;116 (23):4806–4814.
[13] Jung HE, Shim YR, Oh JE, Oh DS, Lee HK. The autophagy protein Atg5 plays a crucial role in the maintenance and reconstitution ability of hematopoietic stem cells. *Immune Netw* 2019;19(2):e12.
[14] Mortensen M, Soilleux EJ, Djordjevic G, et al. The autophagy protein Atg7 is essential for hematopoietic stem cell maintenance. *J Exp Med* 2011;208(3):455–467.
[15] Sahni S, Merlot AM, Krishan S, Jansson PJ, Richardson DR. Gene of the month: BECN1. *J Clin Pathol* 2014;67(8):656–660.
[16] Chang C, Young LN, Morris KL, et al. Bidirectional control of autophagy by BECN1 BARA domain dynamics. *Mol Cell* 2019;73 (2):339–353. e336.
[17] Cao Y, Klionsky DJ. Physiological functions of Atg6/Beclin 1: a unique autophagy-related protein. *Cell Res* 2007;17(10):839–849.
[18] Oberstein A, Jeffrey PD, Shi Y. Crystal structure of the Bcl-XL-Beclin 1 peptide complex: Beclin 1 is a novel BH3-only protein. *J Biol Chem* 2007;282(17):13123–13132.
[19] Kang R, Zeh HJ, Lotze MT, Tang D. The Beclin 1 network regulates autophagy and apoptosis. *Cell Death Differ* 2011;18 (4):571–580.
[20] Wirawan E, Vande Walle L, Kersse K, et al. Caspase-mediated cleavage of Beclin-1 inactivates Beclin-1-induced autophagy and enhances apoptosis by promoting the release of proapoptotic factors from mitochondria. *Cell Death Dis* 2010;1:e18.
[21] Goodall ML, Fitzwalter BE, Zahedi S, et al. The autophagy machinery controls cell death switching between apoptosis and necroptosis. *Dev Cell* 2016;37(4):337–349.
[22] Wu YT, Tan HL, Huang Q, et al. Autophagy plays a protective role during zVAD-induced necrotic cell death. *Autophagy* 2008;4(4):457–466.
[23] Kim TS, Hanak M, Trampont PC, Braciale TJ. Stress-associated erythropoiesis initiation is regulated by type 1 conventional dendritic cells. *J Clin Invest* 2015;125(10):3965–3980.
[24] Tesio M, Trumpp A. Breaking the cell cycle of HSCs by p57 and friends. *Cell Stem Cell* 2011;9(3):187–192.
[25] Li J. Quiescence regulators for hematopoietic stem cell. *Exp Hematol* 2011;39(5):511–520.
[26] Cheng EH, Wei MC, Weiler S, et al. BCL-2, BCL-XL sequester BH3 domain-only molecules preventing BAX- and BAK-mediated mitochondrial apoptosis. *Mol Cell* 2001;8(3):705–711.
[27] Jabbour AM, Heraud JE, Daunt CP, et al. Puma indirectly activates Bax to cause apoptosis in the absence of Bid or Bim. *Cell Death Differ* 2009;16(4):555–563.
[28] Wang J, Lu X, Sakk V, Klein CA, Rudolph KL. Senescence and apoptosis block hematopoietic activation of quiescent hematopoietic stem cells with short telomeres. *Blood* 2014;124(22):3237–3240.

[29] Beerman I, Seita J, Inlay MA, Weissman IL, Rossi DJ. Quiescent hematopoietic stem cells accumulate DNA damage during aging that is repaired upon entry into cell cycle. *Cell Stem Cell* 2014;15(1):37–50.
[30] Walsh JG, Cullen SP, Sheridan C, Luthi AU, Gerner C, Martin SJ. Executioner caspase-3 and caspase-7 are functionally distinct proteases. *PNAS* 2008;105(35):12815–12819.
[31] Zhang Y, Chen X, Gueydan C, Han J. Plasma membrane changes during programmed cell deaths. *Cell Res* 2018;28(1):9–21.
[32] Sun L, Wang H, Wang Z, et al. Mixed lineage kinase domain-like protein mediates necrosis signaling downstream of RIP3 kinase. *Cell* 2012;148 (1–2):213–227.
[33] He WT, Wan H, Hu L, et al. Gasdermin D is an executor of pyroptosis and required for interleukin-1beta secretion. *Cell Res* 2015;25 (12):1285–1298.
[34] Wang Y, Gao W, Shi X, et al. Chemotherapy drugs induce pyroptosis through caspase-3 cleavage of a gasdermin. *Nature* 2017;547(7661):99–103.
[35] Shi J, Zhao Y, Wang K, et al. Cleavage of GSDMD by inflammatory caspases determines pyroptotic cell death. *Nature* 2015;526(7575):660–665.
[36] Heng T, Painter M, Elpek K, et al. The immunological genome project: networks of gene expression in immune cells. *Nat Immunol* 2008;9:1091–1094.
[37] Wu C, Orozco C, Boyer J, et al. BioGPS: an extensible and customizable portal for querying and organizing gene annotation resources. *Genome Biol* 2009;10(11):R130.
[38] Rudin CM, Hann CL, Garon EB, et al. Phase II study of single-agent navitoclax (ABT-263) and biomarker correlates in patients with relapsed small cell lung cancer. *Clin Cancer Res* 2012;18(11):3163–3169.
[39] Kotschy A, Szlavik Z, Murray J, et al. The MCL1 inhibitor S63845 is tolerable and effective in diverse cancer models. *Nature* 2016;538 (7626):477–482.
[40] Rogers C, Fernandes-Alnemri T, Mayes L, Alnemri D, Cingolani G, Alnemri ES. Cleavage of DFNA5 by caspase-3 during apoptosis mediates progression to secondary necrotic/pyroptotic cell death. *Nat Commun* 2017;8:14128.
[41] Zhao YG, Zhang H. Core autophagy genes and human diseases. *Curr Opin Cell Biol* 2019;61:117–125.
[42] Glover K, Li Y, Mukhopadhyay S, et al. Structural transitions in conserved, ordered Beclin 1 domains essential to regulating autophagy. *J Biol Chem* 2017;292(39):16235–16248.
[43] Liao CC, Ho MY, Liang SM, Liang CM. Recombinant protein rVP1 upregulates BECN1-independent autophagy, MAPK1/3 phosphorylation and MMP9 activity via WIPI1/WIPI2 to promote macrophage migration. *Autophagy* 2013;9(1):5–19.
[44] Smith DM, Patel S, Raffoul F, Haller E, Mills GB, Nanjundan M. Arsenic trioxide induces a beclin-1-independent autophagic pathway via modulation of SnoN/SkiL expression in ovarian carcinoma cells. *Cell Death Differ* 2010;17(12):1867–1881.
[45] Gao P, Bauvy C, Souquere S, et al. The Bcl-2 homology domain 3 mimetic gossypol induces both Beclin 1-dependent and Beclin 1-independent cytoprotective autophagy in cancer cells. *J Biol Chem* 2010;285 (33):25570–25581.
[46] Niso-Santano M, Bravo-San Pedro JM, Maiuri MC, et al. Novel inducers of BECN1-independent autophagy: cis-unsaturated fatty acids. *Autophagy* 2015;11(3):575–577.
[47] Scarlatti F, Maffei R, Beau I, Ghidoni R, Codogno P. Non-canonical autophagy: an exception or an underestimated form of autophagy? *Autophagy* 2008;4(8):1083–1085.
[48] Ashkenazi A, Bento CF, Ricketts T, et al. Polyglutamine tracts regulate beclin 1-dependent autophagy. *Nature* 2017;545(7652):108–111.
[49] Peidu Jiang NM. LC3- and p62-based biochemical methods for the analysis of autophagy progression in mammalian cells. *Methods* 2015;75:13–18.
[50] Marx V. Autophagy: eat thyself, sustain thyself. *Nat Methods* 2015;12 (12):1121–1125.
[51] Stankov M, Dimitrova DP, Leverkus M, Klusmann JH, Behrens G. Flow cytometric analysis of autophagic activity with Cyto-ID staining in primary cells. *Bio-protocol* 2014;4(7):e1090.
[52] Kaizuka T, Morishita H, Hama Y, et al. An autophagic flux probe that releases an internal control. *Mol Cell* 2016;64(4):835–849.
[53] Yue Y, Jin S, Yang C, Levine AJ, Heintz N. Beclin 1, an autophagy gene essential for early embryonic development, is a haploinsufficient tumor suppressor. *PNAS* 2003;100(25):15077–15082.
[54] Liang XH, Jackson S, Seaman M, et al. Induction of autophagy and inhibition of tumorigenesis by beclin1. *Nature* 1999;402(9):672–676.
[55] Scarlatti F, Maffei R, Beau I, Codogno P, Ghidoni R. Role of non-canonical Beclin 1-independent autophagy in cell death induced by resveratrol in human breast cancer cells. *Cell Death Differ* 2008;15 (8):1318–1329.
[56] Simsek T, Kocabas F, Zheng J, et al. The distinct metabolic profile of hematopoietic stem cells reflects their location in a hypoxic niche. *Cell Stem Cell* 2010;7(3):380–390.
[57] Liang R, Arif T, Kalmykova S, et al. Restraining lysosomal activity preserves hematopoietic stem cell quiescence and potency. *Cell Stem Cell* 2020;26(3):359–376.e7.
[58] Watanuki S, Kobayashi H, Sorimachi Y, Yamamoto M, Okamoto S, Takubo K. ATP turnover and glucose dependency in hematopoietic stem/progenitor cells are increased by proliferation and differentiation. *Biochem Biophys Res Commun* 2019;514(1):287–294.
[59] Edinger AL, Thompson CB. Death by design: apoptosis, necrosis and autophagy. *Curr Opin Cell Biol* 2004;16(6):663–669.
[60] Zamaraeva MV, Sabirov RZ, Maeno E, Ando-Akatsuka Y, Bessonova SV, Okada Y. Cells die with increased cytosolic ATP during apoptosis: a bioluminescence study with intracellular luciferase. *Cell Death Differ* 2005;12(11):1390–1397.
[61] Leist M, Single B, Castoldi AF, Kühnle S, Nicotera P. Intracellular adenosine triphosphate (ATP) concentration: a switch in the decision between apoptosis and necrosis. *J Exp Med* 1997;185(8):1481–1486.
[62] Croes L, Fransen E, Hylebos M, et al. Determination of the potential tumor-suppressive effects of Gsdme in a chemically induced and in a genetically modified intestinal cancer mouse model. *Cancers (Basel)* 2019;11(8). doi: 10.3390/cancers11081214. 2019-08-20.
[63] Qu X, Yu J, Bhagat G, et al. Promotion of tumorigenesis by heterozygous disruption of the beclin 1 autophagy gene. *J Clin Invest* 2003;112 (12):1809–1820.
[64] Croes L, Beyens M, Fransen E, et al. Large-scale analysis of DFNA5 methylation reveals its potential as biomarker for breast cancer. *Clin Epigenetics* 2018;10:51.
[65] Akino K, Toyota M, Suzuki H, et al. Identification of DFNA5 as a target of epigenetic inactivation in gastric cancer. *Cancer Sci* 2007;98(1):88–95.
[66] Ibrahim J, Op de Beeck K, Fransen E, et al. Methylation analysis of Gasdermin E shows great promise as a biomarker for colorectal cancer. *Cancer Med* 2019;8(5):2133–2145.
[67] Broz P, Pelegrin P, Shao F. The gasdermins, a protein family executing cell death and inflammation. *Nat Rev Immunol* 2020;20(3):143–157.
[68] Wang J, Sun Q, Morita Y, et al. A differentiation checkpoint limits hematopoietic stem cell self-renewal in response to DNA damage. *Cell* 2012;148(5):1001–1014.